Delay and Doppler Profiler based Channel Transfer Function Estimation for 2x2 MIMO Receivers in 5G System Targeting a 500km/h Linear Motor Car

Suguru Kuniyoshi[1)], Rie Saotome[1)], Shiho Oshiro[2)] and Tomohisa Wada[3)]
kuniyoshi@magnadesignnet.com
1) Magna Design Net Inc., 3-1-15 Maejima, Naha-shi, Okinawa, Japan
2) Information Technology Center, University of the Ryukyus, Okinawa, Japan
3) Dept. of Engineering, University of the Ryukyus, Senbaru 1, Nishihara, Okinawa, Japan

Summary
In Japan, high-speed ground transportation service using linear motors at speeds of 500 km/h is scheduled to begin in 2027. To accommodate 5G services in trains, a subcarrier spacing frequency of 30 kHz will be used instead of the typical 15 kHz subcarrier spacing to mitigate Doppler effects in such high-speed transport. Furthermore, to increase the cell size of the 5G mobile system, multiple base station antennas will transmit identical downlink (DL) signals to form an expanded cell size along the train rails. In this situation, the forward and backward antenna signals are Doppler-shifted in opposite directions, respectively, so the receiver in the train may suffer from estimating the exact Channel Transfer Function (CTF) for demodulation. In a previously published paper, we proposed a channel estimator based on Delay and Doppler Profiler (DDP) in a 5G SISO (Single Input Single Output) environment and successfully implemented it in a signal processing simulation system. In this paper, we extend it to 2x2 MIMO (Multiple Input Multiple Output) with spatial multiplexing environment and confirm that the delay and DDP based channel estimator is also effective in 2x2 MIMO environment. Its simulation performance is compared with that of a conventional time-domain linear interpolation estimator. The simulation results show that in a 2x2 MIMO environment, the conventional channel estimator can barely achieve QPSK modulation at speeds below 100 km/h and has poor CNR performance versus SISO. The performance degradation of CNR against DDP SISO is only 6dB to 7dB. And even under severe channel conditions such as 500km/h and 8-path inverse Doppler shift environment, the error rate can be reduced by combining the error with LDPC to reduce the error rate and improve the performance in 2x2 MIMO. QPSK modulation scheme in 2x2 MIMO can be used under severe channel conditions such as 500 km/h and 8-path inverse Doppler shift environment.

Key words:
5G, 5th Generation Mobile Communication System, MIMO, Multiple Input Multiple Output, Channel estimation, Delay and Doppler profiler

I. Introduction

A 500 km/h linear motor high speed terrestrial transportation service is planned to launch 2027 between Tokyo and Nagoya in Japan. The maximum speed of current high speed train Shinkansen is 300 km/h. However, the coming linear motor train's speed will be 500 km/h by using magnetic levitation mechanism. In order to support 5G service in the train, 5G will use some different configurations. First, increased sub-carrier spacing f_0 of 30 kHz is used instead of conventional 15 kHz to mitigate Doppler frequency shift. This change automatically shortens OFDM symbol length by half. Consequently, channel state change tracking performance will increase. Second, to increase mobile service cell size, plural Base Station antennas transmit the identical Downlink (DL) signal to form the expanded cell size along the train rail. In this situation, forward and backward antenna signals will be Doppler shifted by reverse directions respectively and the receiver in the train might suffer to estimate accurate Channel Transfer Function (CTF) for demodulation. Fig. 1 shows the situation of two DL signals reception in the car. Approaching TX1 antenna signal is $+f_d$ shifted and backward TX2 signal is $-f_d$ shifted. In a MIMO system, spatial multiplexing is performed using two or more transmit antennas at the base station. In order to separate the spatially multiplexed signals, two or more antennas of the receiving equipment are also required. In the previous paper [1], the effectiveness of the channel estimation scheme using the Delay and Doppler Profiler (DDP) algorithm was demonstrated by computer simulations in an environment limited to the SISO (Single Input Single Output)

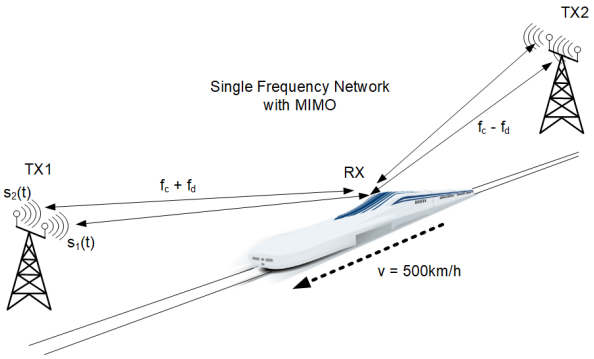

Fig. 1: Reception environment of revised Doppler shifted signals by combining signals originating from two base stations in a single frequency network with MIMO channels in the high-speed train

Manuscript received September 5, 2023
Manuscript revised September 20, 2023
https://doi.org/10.22937/IJCSNS.2023.23.9.2

propagation path. In this paper, we applied the channel estimation using the DDP algorithm to 2x2 MIMO with spatial multiplexing in order to achieve higher transmission data rate, and build a simulation model. In section II, first, targeting 5G Mobile Communication System is briefly shown. Then the proposed DDP method is explained. Computer simulation results are shown in section III. Finally, in section IV, the conclusions will be given.

II. 5G Mobile Communication System MIMO Architecture

5th Generation Mobile Communication System [2] is OFDM communication system standard developed as the successor to the 4G-LTE (4th Generation Long term evolution) system with various enhancements. For example, the sub-carrier spacing was fixed as 15kHz in 4G-LTE but in 5G variable sub-carrier spacing is supported such as 15 / 30 / 60 / 120 / 240 kHz. For the application of the linear motor train, 30 kHz sub-carrier frequency will be used for RF Carrier of 3.9 GHz Band. Table I summaries the 5G system parameters for this application. To support eMBB (enhanced Mobile Broadband), 100MHz bandwidth is assumed with 3276 sub-carriers. Because of sub-carrier spacing f_0 of 30 kHz, OFDM symbol length T of 33.33us (4096 sampling points) is used.

Fig. 2 shows the 5G frame structure when f_0 is 30 kHz. This structure is a Frequency Range 1 frame structure, commonly referred to as Sub6, which is used when the center frequency is below 6 GHz. 1 frame length is 10 ms and divided into 20 Slots. In one Slot, 14 OFDM symbols are embedded. Cyclic prefix (CP) length is 288 sampling points for each 4096 points OFDM symbols except the 1st CP. The length of the 1st CP is a little expanded such as 352 points. In 5G system, Demodulation Reference Signals (DMRS) are inserted to some Sub-carriers to measure CTF and the DMRS can be placed with a high degree of freedom according to the system configuration. This time, DMRS is asserted in S3, S6, S9, S12 OFDM symbols to detect rapidly time-domain changing CTF [3].

Time-Frequency structure of this 5G system is shown in Fig. 3. Since 12 sub-carriers and 14 OFDM symbols constitute one Common Resource Block (CRB), the total 3276 sub-carriers correspond to 273 CRBs. The detail of sub-carrier arrangement in a CRB is also shown in the figure. For frequency direction (vertically), DMRS for Tx Antenna 1 are placed every 2 sub-carriers as shown in the odd number places. Similarly, DMRS for Tx Antenna 2 are placed every 2 sub-carriers as shown in the even number places.

Table 1: 5th Generation Mobile Communication System Parameters

Parameters	Value
System Band Width	100 MHz
Sub-carrier Spacing (f_0)	30 kHz
Pass Band Frequency	3.9 GHz
OFDM symbol length (T)	33.33 us (4096 points)
Number of Common Resource Blok (CRB)	273
Number of Sub-carriers	3276
Sampling Frequency (Fs)	122.88 Msps
FFT size	4096
CP length	352 or 288 points

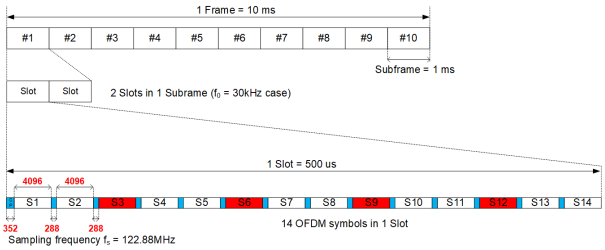

Fig. 2: 5G Frame and Slot structure

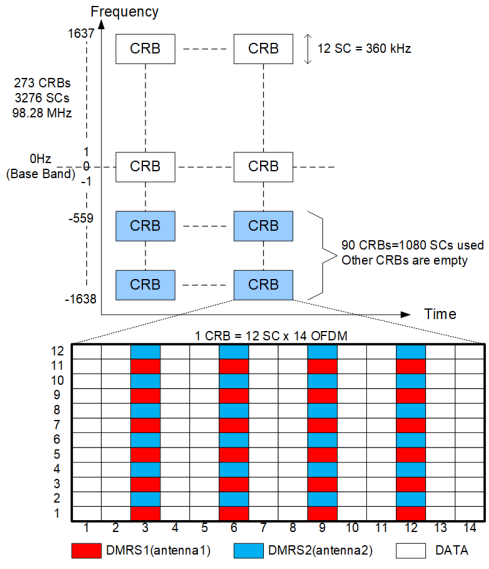

Fig. 3: Time and Frequency structure of 5G System for 2x2 MIMO

A) Physical layer of 5G communication MIMO system

Fig. 4 shows the block diagram of the Physical Layer (PHY) for 5G 2x2 MIMO (Multiple Input Multiple Output) system. The upper side is the transmitter and the lower side is the receiver. The Bit data supplied from the upper MAC (Media Access Control), protocol and application layers are digitally modulated into QPSK / 16QAM / 64QAM / 256QAM at the Antenna mapper, and the modulated symbols are then split as different streams at each of the two transmit antennas as shown in Fig. 4. Then the modulated symbols and DMRS pilot signals for each Tx antennas configured Slots as shown in Fig. 3. Then Inverse 4096 points Fourier Transform (IFFT) is performed as OFDM modulation and CP is appended for each Tx antenna. This signal is Baseband (BB) signals. Up-conversion is applied to the BB signal to generate passband signals, which are radiated through a power amplifiers and antennas for each stream. In this paper, 2x2 MIMO refers to spatial multiplexing MIMO unless otherwise specified. Thus, 2x2 MIMO has twice the transmission capacity compared to SISO.

The receiver side basically performs basically the reverse process of the transmitter side. However, since the receiving signal is distorted through the propagation channel, CTF, which is a Frequency domain representation of Channel Impulse Response in Time domain, has to be estimated and the distortion has to be compensated at Equalizer using the estimated CTF. In addition, signals transmitted separately at the transmitter end arrive at the receiver end after being mixed together on the propagation channel. Therefore, the CTF must be calculated for four paths in 2x2 MIMO environment, compared to the amount of CTF calculations required in SISO environment, which quadruples the amount of calculations required to find the CTF.

Conventional 5G receivers interpolate CTF values measured at DMRS locations in the frequency and time domains to obtain CTFs for all subcarrier locations; in a MIMO environment, channel estimation needs to be more accurate than in a SISO environment. To improve CTF estimation, this paper applies the DDP to 2x2 MIMO with spatial multiplexing environment to study CTF generation method that is more accurate than conventional CTF estimation methods.

B) Improved Channel Transfer Function estimation based on Delay and Doppler Profile for 2x2 MIMO

References [4-6] describe detail methods of Delay and Doppler Profile (DDP) based CTF estimation using pilot signals embedded in OFDM sub-carriers. Fig. 5 is a block diagram of proposed DDP CTF generation. The upper side of the figure represents the Time-Frequency structure

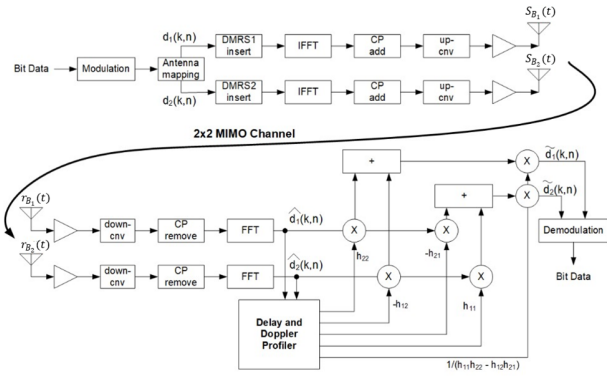

Fig. 4: Physical layer of 5G communication system for 2x2 MIMO

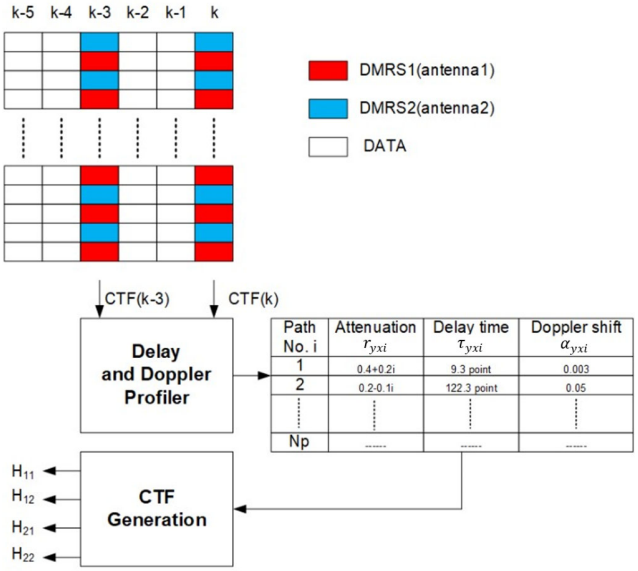

Fig. 5: Delay and Doppler Profiler based CTF estimator for 2x2 MIMO

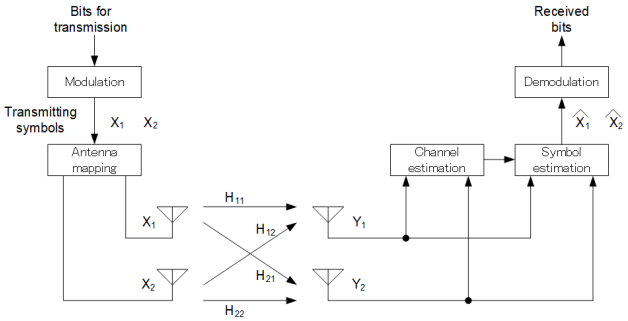

Fig. 6: Basic representation of 2x2 MIMO system

of sub-carriers with time-domain symbol index k. The DDP estimates each N_P, multipath component waves to receiving each antenna. Each analyzed component can be characterized using three parameters such as Attenuation r_{yxi}, Propagation Delay time τ_{yxi}, and normalized Doppler shift α_{yxi} with transmit antenna number x, receive antenna number y, and wave component index i. Here the Attenuation r_{yxi} is complex value including amplitude attenuation and phase rotation and the normalized Doppler shift is normalized by sub-carrier spacing f_0 such as $\alpha_{yxi} = fd_i/f_0$. Using the symbol k measured $CTF_{yx}(k)$ and symbol $k-3$ measured $CTF_{yx}(k-3)$, the DDP detects N_P sets of those three parameters.

5G baseband transmitting for 2x2 MIMO signals $s_{B_1}(t)$ and $s_{B_2}(t)$ can be expressed as Equations (1a) and (1b). As shown in Fig. 4, $s_{B_1}(t)$ represents the signal from transmitting antenna number 1, and $s_{B_2}(t)$ represents the signal from transmitting antenna number 2.

$$s_{B1}(t) = \sum_{m=-\infty}^{\infty} g(t-mT_s) \cdot \sum_{n=0}^{N-1} d_1(m,n) e^{j2\pi n f_0 (t-mT_s)} \quad \cdots (1a)$$

$$s_{B2}(t) = \sum_{m=-\infty}^{\infty} g(t-mT_s) \cdot \sum_{n=0}^{N-1} d_2(m,n) e^{j2\pi n f_0 (t-mT_s)} \quad \cdots (1b)$$

$$T_s = \frac{1}{f_0} + T_g \quad \cdots (2)$$

$$g(t) = \begin{cases} 1 & -T_g \leqq t < 1/f_0 \\ 0 & otherwise \end{cases} \quad \cdots (3)$$

where, N is the number of sub-carriers, f_0 is the sub-carrier spacing, T_s is symbol length as defined in equation (2), $d_1(m,n)$ and $d_2(m,n)$ are data symbols of sub-carrier index n at the m^{th} OFDM symbol. By assuming the transmission channel has N_P delay paths, the received baseband signals can be written as Equations (4a) and (4b).

$$r_{B1}(t) = \sum_{p=1}^{N_P} r_{11p}\, s_{B1}(t-\tau_{11p}) e^{j2\pi\Delta f_{11p}(t-\tau_{11p})} + \sum_{p=1}^{N_P} r_{12p}\, s_{B2}(t-\tau_{12p}) e^{j2\pi\Delta f_{12p}(t-\tau_{12p})} \quad \cdots (4a)$$

$$r_{B2}(t) = \sum_{p=1}^{N_P} r_{21p}\, s_{B1}(t-\tau_{21p}) e^{j2\pi\Delta f_{21p}(t-\tau_{21p})} + \sum_{p=1}^{N_P} r_{22p}\, s_{B2}(t-\tau_{22p}) e^{j2\pi\Delta f_{22p}(t-\tau_{22p})} \quad \cdots (4b)$$

$$t = \frac{i}{Nf_0} + kT_s \quad \cdots (5)$$

where, r_{yxp}, τ_{yxp} and Δf_{yxp} are attenuation, relative delay and Doppler-shift of p^{th} path when the signal from transmit antenna $\#x$ is received at receive antenna $\#y$, respectively. After sampling of $r_{B_1}(t)$ and $r_{B_1}(t)$ by using Equation (5) with sampling index i and OFDM symbol number k, the block of samples is de-modulated by DFT to generate data symbol $\widehat{d_1}(k,l)$ and 1 $\widehat{d_2}(k,l)$ as expressed in Equations (6a) and (6b).

$$\widehat{d_1}(k,l) = h_{11}(k,l,l)d_1(k,l) + \sum_{\substack{n=0 \\ n\neq l}}^{N-1} h_{11}(k,l,n)d_1(k,n) + h_{12}(k,l,l)d_2(k,l) + \sum_{\substack{n=0 \\ n\neq l}}^{N-1} h_{12}(k,l,n)d_2(k,n) + w_1(k,l) \quad \cdots (6a)$$

$$\widehat{d_2}(k,l) = h_{21}(k,l,l)d_1(k,l) + \sum_{\substack{n=0 \\ n\neq l}}^{N-1} h_{21}(k,l,n)d_1(k,n) + h_{22}(k,l,l)d_2(k,l) + \sum_{\substack{n=0 \\ n\neq l}}^{N-1} h_{22}(k,l,n)d_2(k,n) + w_2(k,l) \quad \cdots (6b)$$

where $w_1(k,l)$ and $w_2(k,l)$ are additive noise that corresponds to the l^{th} sub-carrier in the k^{th} OFDM symbol and $h_{yx}(k,l,n)$ is the channel transfer function from symbol $d_1(k,n)$ and $d_2(k,n)$ to the l^{th} sub-carrier. If $n \neq l$, $h_{yx}(k,l,n)$ represents the influence of ICI (Inter Carrier Interference). $h_{yx}(k,l,n)$ can be expressed as Equations (7), (8a) and (8b).

$$h_{yx}(k,l,n) = \sum_{p=1}^{N_P} h_{yxp}(k,l,n) \quad \cdots (7)$$

$$h_{yxp}(k,l,n) = \frac{sinc(A)}{sinc(\frac{A}{N})} \cdot e^{j\frac{\pi(N-1)A}{N}} \cdot r_{yxp} \cdot e^{-j\frac{2\pi(n+\alpha_{yxp})\tau'_{yxp}}{N}} \cdot e^{j\frac{2\pi k(N+GI)\alpha_{yxp}}{N}} \quad \cdots (8a)$$

$$A = n - l + \alpha_{yxp} \quad \cdots (8b)$$

where $\alpha_{yxp} = \Delta f_{yxp}/f_0$ is normalized frequency offset of p^{th} path when the signal from transmit antenna number x is received at receive antenna number y, respectively.

The parameters of channel transfer function $h_{yx}(k,l,n)$ are estimated so as to minimize the mean square error shown in Equation (9).

$$E_{yx}(k) = \sum_{l=\boldsymbol{P}} \left\{ \left| CTF_{yx}(k,l) - h_{yx}(k,l,l) \right|^2 + \left| CTF_{yx}(k-3,l) - h_{yx}(k-3,l,l) \right|^2 \right\} \quad \cdots (9)$$

where $\Sigma_{l=\boldsymbol{P}}$ means that the summation is performed as long as l is DMRS pilot symbol.

In order to simplify the problem, it is supposed that the channel model contains one path at the first. In this case, criterion is rewritten as Equation (10).

$$E_{yx1}(k) = \sum_{l=P}\left\{\left|CTF_{yx}(k,l) - f(\alpha_{yx1})r_{yx1}\cdot e^{-j\frac{2\pi(l+\alpha_{yx1})\tau'_{yx1}}{N}}\right|^2 + \left|CTF_{yx}(k-3,l) - f(\alpha_{yx1})r_{yx1}\cdot e^{-j\frac{2\pi(l+\alpha_{yxp})\tau'_{yx1}}{N}}\cdot e^{j\frac{-2\pi3(N+GI)\alpha_{yx1}}{N}}\right|^2\right\} \quad \cdots(10)$$

here, $f(\alpha_{yx1})$ is written as Equation (11).

$$f(\alpha_{yx1}) = \frac{sinc(\alpha_{yx1})}{sinc\left(\frac{\alpha_{yx1}}{N}\right)}\cdot e^{j\frac{\pi(N-1)\alpha_{yx1}}{N}}\cdot e^{j\frac{2\pi k(N+GI)\alpha_{yx1}}{N}} \quad \cdots(11)$$

One of the necessary conditions to minimize $E_{yx1}(k)$ with regard to r_{yx1}, τ'_{yx1} (relative delay time in sampling points) and α_{yx1} is that its partial derivative of r_{yx1} has zero value. With this condition, r_{yx1} can be shown as Equations (12a) and (12b).

$$r_{yx1} = \frac{S^*_{yx\_k} + e^{j\frac{2\pi3(N+GI)\alpha_{yx1}}{N}}S^*_{yx\_k-3}}{2\cdot f(\alpha_{yx1})e^{-j\frac{2\pi\alpha_{yx1}\tau'_{yx1}}{N}}} \quad \cdots(12a)$$

here,

$$S_{yx\_k} = \sum_{l=P} CTF^*_{yx}(k,l)\, e^{-j\frac{2\pi l\tau'_{yx1}}{N}} \quad \cdots(12b)$$

By calculate more as shown in references [4-6], α_{yx1} is calculated from τ'_{yx1} as Equation (13).

$$\alpha_{yx1} = \frac{1}{\frac{2\pi3(N+GI)}{N}} arctan\left|\frac{\Im(S^*_{yx\_k}\cdot S_{yx\_k-3})}{\Re(S^*_{yx\_k}\cdot S_{yx\_k-3})}\right| \quad \cdots(13)$$

Consequently, once τ'_{yx1} is determined, r_{yx1} and α_{yx1} are easily obtained from Equations (12a) and (13), respectively. In this proposed method, τ'_{yx1} is changed by $1/(2Nf_0)$ (twice of sampling frequency) and rough estimation is first obtained. And this rough estimation is modified to more precise value using Newton method as described in references [4-6].

According to the computation above, $h_{yx1}(k,l,n)$ can be obtained using Equations (8a) and (8b). Then, measured $CTF_{yx}(k,l)$ and $CTF_{yx}(k-3,l)$ are updated to $CTF_{yx}(2,k,l)$ and $CTF_{yx}(2,k-3,l)$ by subtracting $h_{yx1}(k,l,n)$ and $h_{yx1}(k-3,l,n)$ respectively. By removing the influence of the first estimated path from the cost function $E_{yx1}(k)$, the following criterion $E_{yx2}(k)$ can be obtained such as Equation (14).

$$E_{yx2}(k) = \sum_{l=P}\left\{\left|CTF_{yx}(2,k,l) - f(\alpha_{yx1})r_{yx1}\cdot e^{-j\frac{2\pi(l+\alpha_{yx1})\tau'_{yx1}}{N}}\right|^2 + \left|CTF_{yx}(2,k-3,l) - f(\alpha_{yx1})r_{yx1}\cdot e^{-j\frac{2\pi(l+\alpha_{yxp})\tau'_{yx1}}{N}}\cdot e^{j\frac{-2\pi3(N+GI)\alpha_{yx1}}{N}}\right|^2\right\} \quad \cdots(14)$$

Since $E_{yx2}(k)$ contains the influence of other paths, the second path can be estimated using the same procedure in the previous section. By repeating this operation by the number of paths in the channel model, N_p sets of those three parameters can be obtained as shown in Fig. 5, and Fig. 6.

The CTF needs to be calculated for the number of combinations of the number of transmit and receive antennas. Therefore, in the case of 2x2 MIMO, the number of CTF calculations is required for four paths H_{11}, H_{12}, H_{21} and H_{22} as shown in Fig. 6. This can be expressed in the theoretical equation as shown in Equation (15) below.

$$\begin{bmatrix}Y_1\\Y_2\end{bmatrix} = \begin{bmatrix}H_{11} & H_{12}\\H_{21} & H_{22}\end{bmatrix}\begin{bmatrix}X_1\\X_2\end{bmatrix} + \begin{bmatrix}n_1\\n_2\end{bmatrix} \quad \cdots(15)$$

The equation for channel equalization using the channel estimation results of the received signal is shown in Equation (16).

$$\begin{bmatrix}\widehat{X_1}\\\widehat{X_2}\end{bmatrix} \cong \begin{bmatrix}H_{11} & H_{12}\\H_{21} & H_{22}\end{bmatrix}^{-1}\begin{bmatrix}Y_1\\Y_2\end{bmatrix} \quad \cdots(16)$$

Now, if we revise that ICI does not occur, Equations (6a) and (6b) can be rewritten as follows.

$$\widehat{d_1}(k,l) = h_{11}(k,l,l)d_1(k,l) + h_{12}(k,l,l)d_2(k,l) + w_1(k,l) \quad \cdots(17a)$$
$$\widehat{d_2}(k,l) = h_{21}(k,l,l)d_1(k,l) + h_{22}(k,l,l)d_2(k,l) + w_2(k,l) \quad \cdots(17b)$$

Equations (17a) and (17b) can also be rewritten using the matrix as follows.

$$\begin{bmatrix}\widehat{d_1}(k,l)\\\widehat{d_2}(k,l)\end{bmatrix} \cong \begin{bmatrix}h_{11}(k,l,l) & h_{12}(k,l,l)\\h_{21}(k,l,l) & h_{22}(k,l,l)\end{bmatrix} \times \begin{bmatrix}d_1(k,l)\\d_2(k,l)\end{bmatrix} \quad \cdots(18)$$

The equalizer of the 2x2 MIMO receiver can be equated as follows. Using the DDP algorithm, Attenuation r_i, Propagation Delay time τ_i, and normalized Doppler shift α_i for wave component index i of the arrival path of each receiving antenna are determined and used as CTFs $H_{11}(k,l,l)$, $H_{12}(k,l,l)$, $H_{21}(k,l,l)$ and $H_{22}(k,l,l)$. Since this paper assumes use in 2x2MIMO, the inverse matrix is calculated by applying the formulas, resulting in the following Equations (19) and (20).

$$\begin{bmatrix}\widehat{d_1}(k,l)\\\widehat{d_2}(k,l)\end{bmatrix} = \frac{1}{\det(\boldsymbol{H})}\begin{bmatrix}h_{22}(k,l,l) & -h_{12}(k,l,l)\\-h_{21}(k,l,l) & h_{11}(k,l,l)\end{bmatrix} \times \begin{bmatrix}\widehat{d_1}(k,l)\\\widehat{d_2}(k,l)\end{bmatrix} \quad \cdots(19)$$

$$\det(\boldsymbol{H}) = h_{11}(k,l,l)h_{22}(k,l,l) - h_{12}(k,l,l)h_{21}(k,l,l) \quad \cdots(20)$$

III. Computer Simulations

Since the actual test environment is not yet available, computer simulations were used to simulate the environment. Fig. 7 shows a computer simulated running linear motor train situation. Nearby Base Station (gNB: g Node B in 5G notation) antennas are located from the train rail by D (m). In a Single Frequency Network (SFN), the same DL signal is transmitted from antennas in different each gNB. The distance between the center of the two Tx antennas of the gNB and the center of the two Rx antennas at the receiver is 300 m. The center position of the two Rx antennas is Xr(t) on the horizontal X axis as shown in Fig. 7. Also, the distance between the Tx antennas is defined as td, and the distance between the Rx antennas is defined as rd. The distances between two Tx antennas and the Rx antenna are $L1_{yx}(t)$, and $L2_{yx}(t)$ $(y = 1,2, x = 1,2)$ as shown in the figure (Fig. 7).

More detail of simulation parameters is listed in Table 2. Assumed Radio passband frequency is 3.9 GHz. In the simulation, moving train will start receiving 1 frames of DL signal with Xr(t=0) = -50 m. Path1-4 DL signal comes from forward antenna with varying length $L1_{11}(t)$, $L1_{12}(t)$, $L1_{21}(t)$, $L1_{22}(t)$ with relative amplitude gain = 1.0. Path5-8 DL signal comes from backside with $L2_{11}(t)$, $L2_{12}(t)$, $L2_{21}(t)$, $L2_{22}(t)$ distance with relative amplitude gain = 0.5. Bit Error Rate (BER) is measured in lower frequency 90 CRBs as shown in Fig. 3. The BER was obtained by adding Additive White Gaussian Noise (AWGN) to the signal received as a composite wave of the 2gNB-derived DL signal, varying from -10 dB to 50 dB in 2 dB steps.

Simulated results for QPSK / 16QAM / 64QAM / 256QAM BER with Carrier to Noise Ratio (CNR) were shown in Figs. 8-11. In each figure, (a) corresponds to conventional linearly interpolated CTF estimation and (b) corresponds to proposed DDR based CTF estimation. Figs. 12-15 show BER vs. train moving speed for QPSK with CNR=22dB, 16QAM with CNR=30dB, 64QAM with CNR=38dB and 256QAM with CNR=46dB.

Assuming that error correction is possible by the error correction mechanism if the BER is less than 1.0E-03, QPSK modulation can be used under severe channel conditions such as 500 km/h under 8-path inverse Doppler shift conditions with the channel estimator using the DDP algorithm based on the proposed method. In the case of 16QAM modulation, the approximate 100 km/h limit is extended to double the speed 200 km/h. 64QAM can only be used in stationary conditions with the conventional method, while the proposed method can be improved to 100 km/h. In the case of 256QAM modulation, only a slight improvement has been observed.

Table 2: Simulation Parameters

Parameters	Value
RF passband frequency	3.9 GHz
Modulation	QPSK / 16QAM / 64QAM / 256QAM
RX moving speed	0 km/h ~ 500km/h, (100km/h step)
CNR	Add to AWGN -10 dB ~ 50 dB, (2 dB step)
Number of Frames	1 Frames (10 ms, 20 slots)
Used number of CRBs	90 CRBs (1080 Sub-carriers)
Channel	2x2 MIMO with Spatial Multiplexing, 8-path Single Frequency Network
Path Group 1 ($L1_{11}(t)$, $L1_{12}(t)$, $L1_{21}(t), L1_{22}(t)$)	Distance = ~50 meters Amp gain = 1.0
Path Group 2 ($L2_{11}(t)$, $L2_{12}(t)$, $L2_{21}(t), L2_{22}(t)$)	Distance = ~250 meters Amp gain = 0.5
Tx Antenna Installation Height (D)	D = 2.0 meters
Tx Antenna Distance (td)	td = 0.5 meters
Rx Antenna Distance (rd)	rd = 0.05 meters

Focusing on the contrast with SISO with QPSK modulation, in 2x2 MIMO environment, conventional channel estimator can barely achieve QPSK modulation below 100 km/h, and the performance of CNR against SISO is poor [1]. DDP based 2x2 MIMO equalizer has a performance degradation of CNR against DDP SISO is only 6dB to 7dB, and combined with LDPC decoder, the error rate can be reduced and performance can be improved in 2x2 MIMO even under severe channel conditions such as 500km/h, 8-path inverse Doppler shift environments.

Fig. 16 shows a graph comparing BER vs. CNR under the same throughput. Since QPSK can transmit a maximum of 2 bits per carrier and 16QAM can transmit a maximum of 4 bits per carrier, the throughput of 16QAM SISO and QPSK 2MIMO with spatial multiplexing is equivalent. From Fig. 16 shows that the proposed QPSK 2MIMO transmission has a lower error rate than the conventional 16QAM SISO transmission.

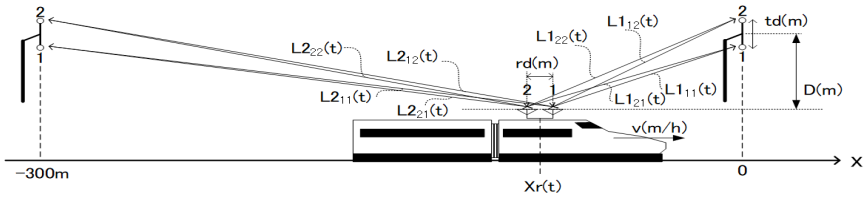

Fig. 7: Simulation model of train moving situation for 2x2 MIMO environment

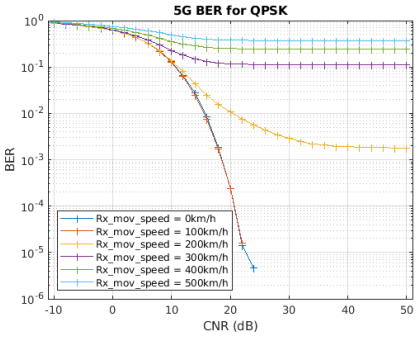

(a) Conventional CTF Linear Interpolator

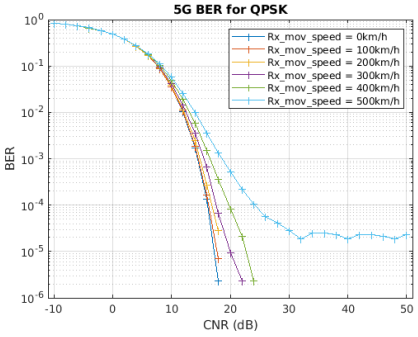

(b) Delay and Doppler Profiler based CTF

Fig. 8: BER vs. CNR (dB) for 2x2 MIMO QPSK modulation

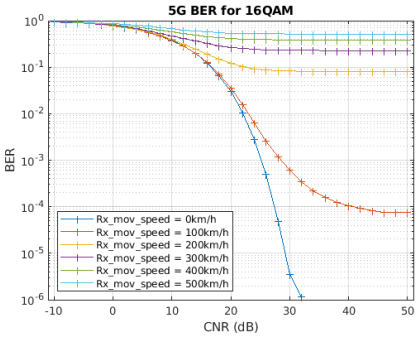

(a) Conventional CTF Linear Interpolator

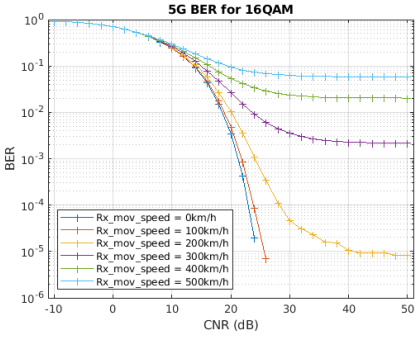

(b) Delay and Doppler Profiler based CTF

Fig. 9: BER vs. CNR (dB) for 2x2 MIMO 16QAM modulation

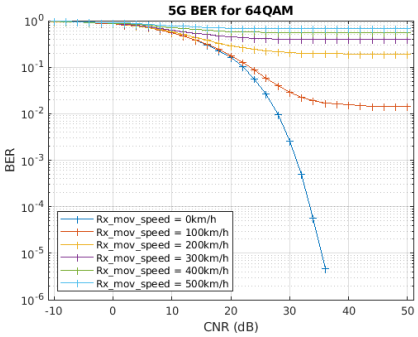

(a) Conventional CTF Linear Interpolator

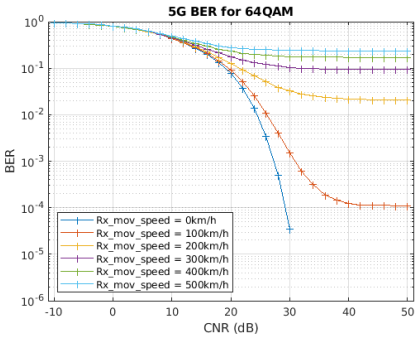

(b) Delay and Doppler Profiler based CTF

Fig. 10: BER vs. CNR (dB) for 2x2 MIMO 64QAM modulation

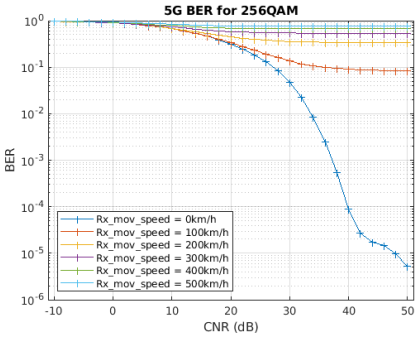

(a) Conventional CTF Linear Interpolator

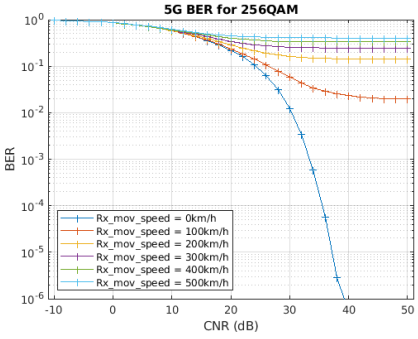

(b) Delay and Doppler Profiler based CTF

Fig. 11: BER vs. CNR (dB) for 2x2 MIMO 256QAM modulation

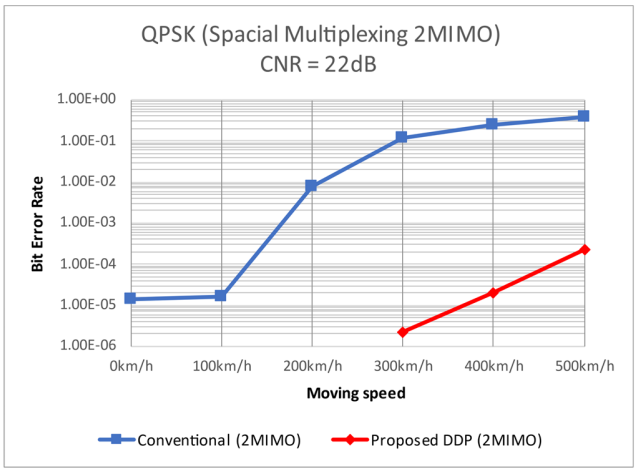

Fig. 12: BER vs. Moving Speed for QPSK

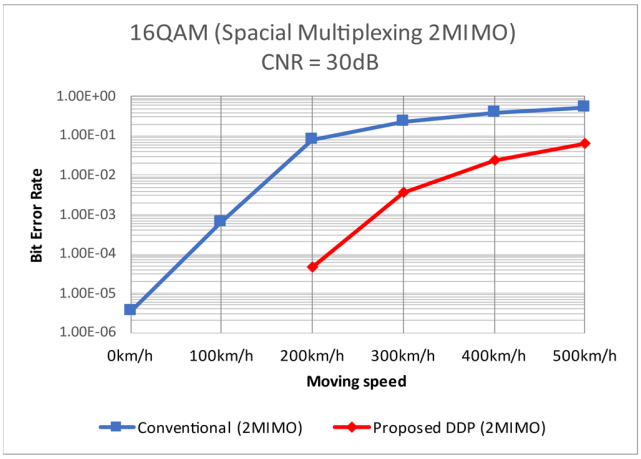

Fig. 13: BER vs. Moving Speed for 16QAM

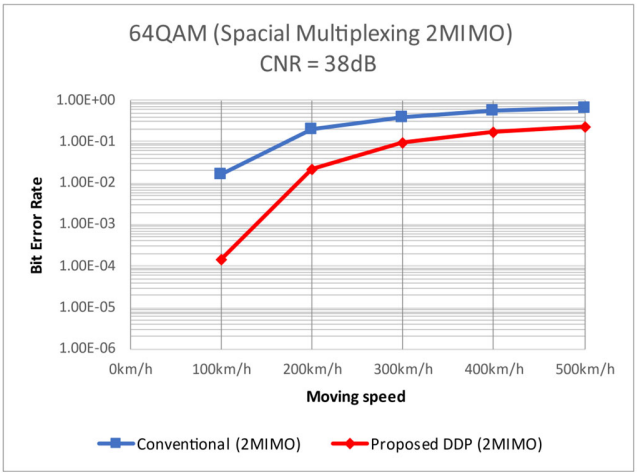

Fig. 14: BER vs. Moving Speed for 64QAM

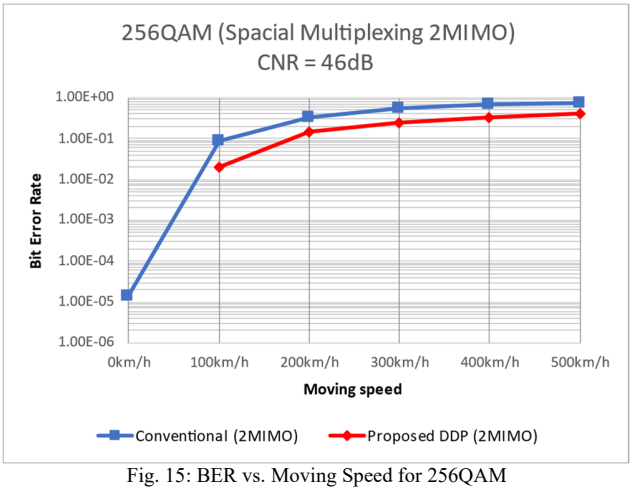

Fig. 15: BER vs. Moving Speed for 256QAM

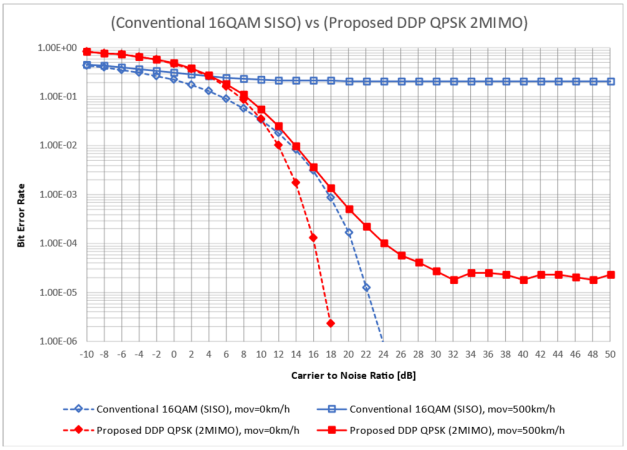

Fig. 16: BER vs. CNR evaluated in terms of the same modulation bit rate

IV. Conclusion

We have proposed Delay and Doppler Profiler (DDP) based channel estimator and successfully implemented it in a computer simulation of a signal processing simulation system for a 500 km/h train. In the simulations, we compared the performance of the proposed DDP algorithm with that of a conventional channel estimation algorithm that combines frequency-domain filter interpolation and time-domain linear interpolation. According to the simulation results, QPSK modulation can be used under severe channel conditions such as 500 km/h under 8-path inverse Doppler shift conditions with the channel estimator using the DDP algorithm based on the proposed method. For 16QAM modulation, roughly 100km/h limitation is extended to double speed of 200km/h. For 64QAM modulation, the limitation speed is improved from below 100km/h. For 256QAM modulation, only small improvement has been confirmed.

We have also shown that the proposed method of transmission with QPSK 2MIMO with spatial multiplexing has a lower error rate than the conventional method of 16QAM SISO.

References

[1] Suguru Kuniyoshi, Shiho Oshiro, Gennan Hayashi, and Tomohisa Wada, "Channel Transfer Function estimation based on Delay and Doppler Profiler for 5G System Receiver targeting 500km/h linear motor car," IJCSNS International Journal of Computer Science and Network Security, VOL.23, No.5, pp.121-127, May 2023.

[2] 3GPP TS38.211 V17.4.0: "3rd Generation Partnership Project; Technical Specification Group Radio Access Network; NR; Physical channels and modulation" Dec. 2022.

[3] Erik Dahlman, Stefan Parkvall, Johan Sköld (2021). *5G NR THE NEXT GENERATION WIRELESS ACCESS TECHNOLOGY SECOND EDITION.* Academic Press.

[4] Mitsuru Nakamura, Makoto Itami, Kohji Itoh and Hamid Aghvami, "ICI Cancellation Technique based on Estimating Delay and Doppler Profile in OFDM Reception," The Institute of Image Information and Television Engineers, Vol. 56, No. 12, pp.1951-1958 (2002).

[5] Mitsuru Nakamura, Masahiro Fujii, Makoto Itami and Kohji Itoh, "MMSE ICI Canceller for OFDM Mobile Reception," The Institute of Image Information and Television Engineers, Vol. 58, No. 1, pp.83-90 (2004).

[6] Akito Yamazaki, Mitsuru Nakamura, Masahiro Fujii, Makoto Itami, Kohji Itoh and Hiroki Ohta, "A Study on Improving Performance of an OFDM ICI Canceller," The Institute of Image Information and Television Engineers, Vol. 58, No. 1, pp.94-101 (2005).

Suguru Kuniyoshi received the B.E. and M.E. degrees, from the University of the Ryukyus, Okinawa, Japan in 2004 and 2006, respectively. He joined Magna Design Net, Inc. in 2006 and has engaged with digital signal processing design of modulator and demodulator part for a Wireless LAN, WiMAX, 4G-LTE, 5G-NR, and Underwater Acoustic communication. Currently he is the Engineering Manager of the Development Department at Magna Design Net, Inc.

Rie Saotome received the B.E. and M.E. degree from Tokyo University of technology, Tokyo, Japan in 1999 and 2001, respectively. She received Dr. Eng. degree from University of the Ryukyus in 2016. From 2004 to 2016, she was a part-time lecturer at Univ. of the Ryukyus, Okinawa Univ., Meio Univ. and Okinawa Polytechnic College. She joined Magna Design Net, Inc. in 2016. Her research interest includes Wireless communications systems, 5G-NR, Underwater Acoustic communication, and Rain attenuation.

Shiho Oshiro received the B.E. and M.E. degrees, from the University of the Ryukyus, Okinawa, Japan in 2018 and 2020, respectively. She received the Dr. Eng. degree from University of the Ryukyus in 2023. She has been an assistant professor at University of the Ryukyus since 2023. She has experienced short-term study abroad at Madan Mohan Malaviya University of Technology (MMMUT) Gorakhpur and Atal Bihari Vajpayee-Indian Institute of Information Technology and Management (ABV-IIITM) Gwalior in India, Institute of Technology of Cambodia (ITC) in Cambodia, and National Taiwan University of Science and Technology (Taiwan Tech). Her research interest includes Underwater OFDM Acoustic communication systems, developed Underwater Acoustic OFDM wireless communication systems, Underwater Acoustic Positioning systems targeting for Underwater Drone controls, Flight Control for Underwater Drone automatically controls, and Autoencoder for OFDM communication system.

Tomohisa Wada received B.S. degree in electronic engineering from Osaka University, Osaka, Japan, in 1983, M.S.E.E. degree from Stanford University, Stanford CA, in 1992, and Ph.D. in electronic engineering from Osaka University in 1994. He joined the ULSI Laboratory, Mitsubishi Electric Corp. Japan in 1983 and engaged in the research and development of VLSI such as High-speed Static Random-access memories, Cache memories for Intel MPUs in 16 years. Since 2001, he has been a Professor at the Department of Information Engineering, the University of the Ryukyus, Okinawa, Japan. In 2001, He was the founding member of Magna Design Net, Inc., which is a fab-less LSI design Company for communication related digital signal processing such as OFDM. Currently, he is also the chief scientist of Magna Design Net, Inc. who is engaging in the research and development of a terrestrial video broadcasting receiver, a wireless LAN, WiMAX, 4G-LTE and 5G systems. After 2009, he also started Underwater OFDM Acoustic communication systems and developed Underwater Acoustic OFDM wireless communication systems and Underwater Acoustic Positioning systems targeting for Underwater Drone controls.